

## Chaos regularization of quantum tunneling rates

Louis M. Pecora,<sup>1</sup> Hoshik Lee,<sup>2</sup> Dong-Ho Wu,<sup>1</sup> Thomas Antonsen,<sup>3</sup> Ming-Jer Lee,<sup>3</sup> and Edward Ott<sup>3</sup>

<sup>1</sup>*Materials Physics and Sensors, US Naval Research Laboratory, Washington, DC 20375, USA*

<sup>2</sup>*Department of Physics, College of William & Mary, Williamsburg, Virginia 23187, USA*

<sup>3</sup>*Physics and Electrical Engineering Departments, University of Maryland, College Park, Maryland 20742, USA*

(Received 29 November 2010; published 13 June 2011)

Quantum tunneling rates through a barrier separating two-dimensional, symmetric, double-well potentials are shown to depend on the classical dynamics of the billiard trajectories in each well and, hence, on the shape of the wells. For shapes that lead to regular (integrable) classical dynamics the tunneling rates fluctuate greatly with eigenenergies of the states sometimes by over two orders of magnitude. Contrarily, shapes that lead to completely chaotic trajectories lead to tunneling rates whose fluctuations are greatly reduced, a phenomenon we call regularization of tunneling rates. We show that a random-plane-wave theory of tunneling accounts for the mean tunneling rates and the small fluctuation variances for the chaotic systems.

DOI: [10.1103/PhysRevE.83.065201](https://doi.org/10.1103/PhysRevE.83.065201)

PACS number(s): 05.45.Mt, 73.40.Gk, 03.65.Xp, 03.75.Lm

Quantum mechanics and classical mechanics have qualitatively different attributes, yet according to the correspondence principle, they should coincide in the limit of small quantum wavelength. This supposed correspondence is particularly intriguing when the classical dynamics of a quantum system is chaotic, since the defining attribute of classical chaos, namely, exponential sensitivity of orbits to small perturbations, does not have a clear quantum counterpart. Thus it is of fundamental interest to explore generic short-wavelength signatures distinguishing the quantum behavior of systems whose classical counterparts yield chaos from those whose classical counterparts are integrable [1]. Here we examine the symmetric/antisymmetric splitting of energy levels in quantum-dot-type systems that are weakly coupled through a tunneling barrier. Since tunneling and energy levels are uniquely quantum concepts, the impact of chaotic vs integrable classical dynamics on quantum behavior is especially relevant and has received much previous attention [2,3]. Our studies reveal a particularly striking distinction between the short-wavelength quantum behavior of classically chaotic and classically integrable systems: Energy level splitting in the classically integrable system can have enormous fluctuations, while in contrast, when the classical system is chaotic, these extreme fluctuations are absent. Our theoretical analysis of this phenomenon uses a previously formulated, correspondence-principal-based concept [4] that gives a statistical characterization of the quantum eigenfunctions of classically chaotic systems.

We examine several, differently shaped, two-dimensional (2D), flat-potential, symmetric, double-well systems in which the two wells are separated by tunneling barriers that run along most of one side of each well. We refer to the difference in energies between a symmetric and antisymmetric pair of states as the tunneling rate, and we denote this difference  $\Delta E$ . For integrable wells the tunneling rates can differ by several orders of magnitude for states that are very close in energy. However, as we move to systems with ubiquitous chaos, at short wavelength the variation of the tunneling rates with energy decreases to a narrow range. We show here that a theory based on ergodicity of classical chaotic orbits in combination with the correspondence principle quantitatively explains this striking phenomenon.

We note that several other works have focused on tunneling rates for dynamical tunneling [3,5]. These consider tunneling between regular and chaotic portions of phase space in some cases where there are local modes in each portion of phase space that are degenerate. They approach the problem using a random matrix approximation of the wave function in the chaotic portion, which is similar in spirit to our method below. In particular, Löck *et al.* [3] show that dynamical tunneling rates can vary by several orders of magnitude depending on the allowed routes between torus islands and the chaotic sea. Our work here differs in that we examine the differences in potential barrier tunneling rates for regular as compared to chaotic well shapes as a function of eigenstate energy.

We numerically solve Schrödinger's equation in the Helmholtz form,  $(\nabla^2 + k^2)\psi(\mathbf{r}) = 0$ , where  $k = \sqrt{E - V}$ ,  $E$  is the eigenstate energy, and  $V$  is the potential energy ( $V = 0$  in the wells,  $V = V_b > E$  in the barrier region, and  $V = \infty$  elsewhere). We take  $\hbar^2/2m = 1$  so all energies are in inverse-length-squared units. Energy level differences are determined to within 1% or smaller accuracy. We calculated all eigenenergies and states from the ground state up to an energy of approximately 800 (just below the barrier potential). This gives about 600 states per double-well system or about 300 symmetric-antisymmetric pairs. Figures 1(a) and 1(b) show the tunneling rates for two extreme cases as a function of the mean energy of the splitting pairs along with some typical eigenstates. Figure 1(a) plots the tunneling rates for a rectangular double-well system. This is one of the few two-dimensional systems that can be solved in closed form. While the tunneling rate is often thought to be determined by the energy, the tunneling rates actually depend directly on the momentum  $p_x$  normal to the barrier. Here  $p_x$  and  $p_y$  in the wells are good labels for each state, and only the  $p_x$  value affects the tunneling rate. This results in horizontal lines of equal-valued tunneling rates for states that all have the same  $p_x$  value but different  $p_y$  values and, hence, energies. It is surprising to see that the tunneling rates for eigenstates of almost equal energy can be vastly different by ratios of over two orders of magnitude. The two wave functions in the inset of Fig. 1(a) show two extremes of this; on the left  $p_y$  is maximal, but for an energetically nearby state on the right,  $p_x$  is maximal. In Fig. 1(b) we show tunneling rates for concave-walled double

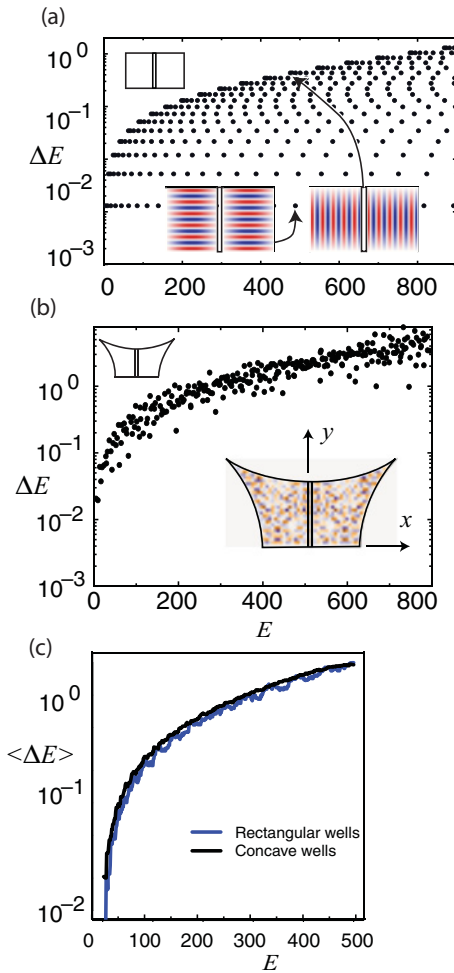


FIG. 1. (Color online) Tunneling rates for integrable and chaotic wells and their sliding averages. Rates for (a) a two-dimensional integrable well, (b) a two-dimensional chaotic well, and (c) their sliding averages. Insets show the double-well and barrier configuration (not to scale) and some typical eigenstates. For the rectangular well (a) low tunneling and high tunneling rate states are shown. The sliding average window width in  $E$  used for (c) is  $4k$ . Parameters [see Fig. 2(a) for definitions] used for both (a) and (b) are  $\Delta = 0.1$ ,  $L = 2.4$ ,  $V_b = 1000$ , and  $A = 4.8$ .

wells. This system is strongly chaotic [6]. In contrast with Fig. 1(a), the tunneling rates as a function of doublet energies is approximately within a factor of 2 for neighboring states—a decrease of two orders of magnitude from Fig. 1(a).

Thus, despite the common intuitive association of classical chaos with enhanced uncertainty and randomness, we see that the opposite appears to prevail in our quantum tunneling problem. Further, in contrast to the extreme difference in the fluctuation characteristics between the classically regular and chaotic systems, we also find that there is an equally striking similarity between them when averaged behavior (rather than fluctuations) is considered. This is illustrated in Fig. 1(c), which shows sliding averages,  $\langle \Delta E \rangle$ , of the data for both the integrable example of Fig. 1(a) and the chaotic example of Fig. 1(b). It is seen that these sliding averages agree well. We now outline our theory quantitatively explaining this contrast between fluctuational and averaged tunneling

behavior in classically chaotic and regular systems (a more detailed version of the theory below will be shown in a future publication [7]).

We consider the situation shown in Fig. 2(a), assuming that the splitting  $\Delta E$  is small compared to the spacing between adjacent energy levels. This allows us to treat the problem using standard perturbation theory, which yields an expression for  $\Delta E$  in terms of an unperturbed eigenfunction  $\psi_0$ . To apply this perturbation theory result we need information on the unperturbed eigenfunction  $\psi_0$ . To obtain this information, we work in the semiclassical regime and make use of the classical chaos and the correspondence principle.

In the classical limit, particle orbits in the well of Fig. 2(a) move with constant speed along straight lines, experiencing specular reflection at the well boundaries, and these orbits are chaotic. As a consequence of this chaos, if we consider a very long typical orbit examined at a randomly chosen instant of time, (i) the probability density of the orbit location within

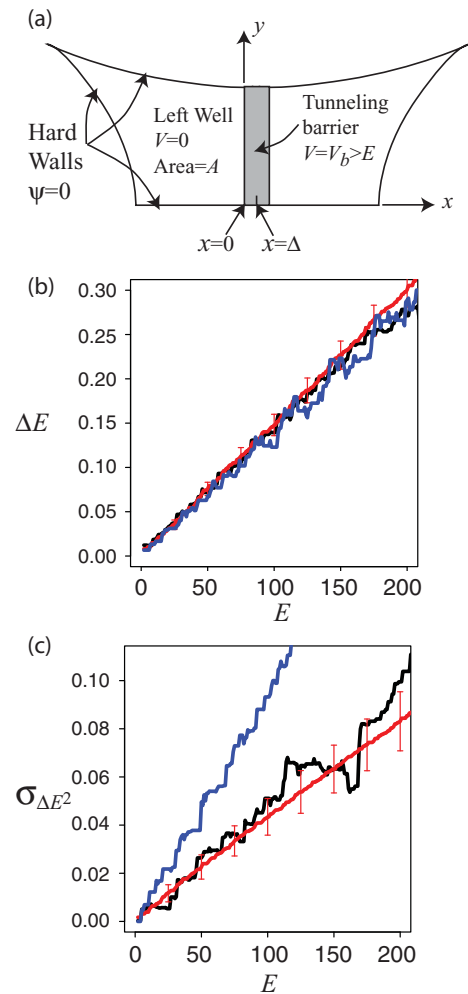


FIG. 2. (Color online) Well coordinates and tunneling rates. The coordinates for the theory are shown in (a). The sliding averages of the splittings are shown in (b) for the theory (red) and for the data from calculations of the concave wells (black) and the rectangular wells (blue). The standard deviations of the tunneling rates are shown in (c) for the theory (red), bowtie wells (black), and rectangular wells (blue).

the well is spatially uniform and (ii) the probability density for the direction of orbit motion is isotropic in angle. These characteristics of the classical orbits that lead to the following properties suggest, through the correspondence principle, the following semiclassical hypothesis for the character of the wave function  $\psi_0$ : (i) the coarse-grained average of  $\psi_0^2$  over regions small compared to the well dimensions, but large compared to wavelength, is approximately uniform in space within the well, and (ii) at any given point in the well interior,  $\psi_0$  has the local character of an isotropic superposition of plane waves. Berry [4], who introduced this idea, has called it the random-plane-wave hypothesis.

Using the random-plane-wave hypothesis we arrive at the following approximate statistical model for the splittings:

$$\Delta E = \sum_{m=1}^{m_*} w_m \Delta_m, \quad (1)$$

where  $w_m > 0$  are random weights satisfying the normalization  $\sum w_m = 1$ ,  $\Delta_m$  is the splitting that applies for a state of the rectangle [Fig. 1(a)] with vertical wave number  $k_y = m\pi/L$  with the same area and barrier parameters ( $L$ ,  $\Delta$ ,  $V_b$ ) as the chaotic well, and  $m_*$  is the integer part of  $kL/\pi$  (i.e.,  $L$  is measured in half-wavelengths, where  $L$  is the barrier length in the  $y$  direction), which is large in the semiclassical limit. As will be shown in our planned subsequent publication [7] the weights are given in terms of  $m_*$ -independent, Gaussian, random variables with zero mean and unit variance.

We have called Eq. (1) a “statistical model” by which we mean the following: Even though the splittings for the chaotic well shown in Fig. 1(b) are deterministic, we regard them as pseudorandom. At any given energy  $E$ , we can use (1) to generate a random  $\Delta E$  by making a random choice for the  $m_*$  Gaussian variables. Our claim is that the statistics of these randomly generated  $\Delta E$  are similar to those of the pseudorandom  $\Delta E$  splitting values obtained via solution of the wave equation. We test this numerically. We use (1) to generate “pseudodata”: for every value of  $E$  corresponding to one of the points plotted in Fig. 1(b), we use (1) to generate a value of  $\Delta E$ . We then statistically compare the actual data with the pseudodata, both for its sliding average [as in Fig. 1(c)] as well as for its fluctuation characteristics.

Figure 2(b) shows the sliding average  $\langle \Delta E \rangle$  obtained from the data in Figs. 1(a) and 1(b) and plotted in Fig. 1(c) as the black and blue curves, along with what we obtain applying the same sliding average procedure to one pseudodata random realization (the red curve). They are seen to be nearly equal.

Equation (1) also suggests an explanation of our observation from Fig. 1(c) that the sliding averages of the chaotic and regular cases are the same. We first note that according to our derivation (appearing in Ref. [7]), the weights  $w_m$  appearing in Eq. (1) have averages corresponding to an isotropic angular distribution of incident plane waves on the barrier. Furthermore, if the sliding average for the rectangle includes a sufficient number of modes in the averaging window, then it reduces to the same isotropic incident angle averaging as in the chaotic case. We consequently expect the two sliding averages to be the same as observed in Fig. 1(c). The above also provides for the understanding of the reduced fluctuation level in the

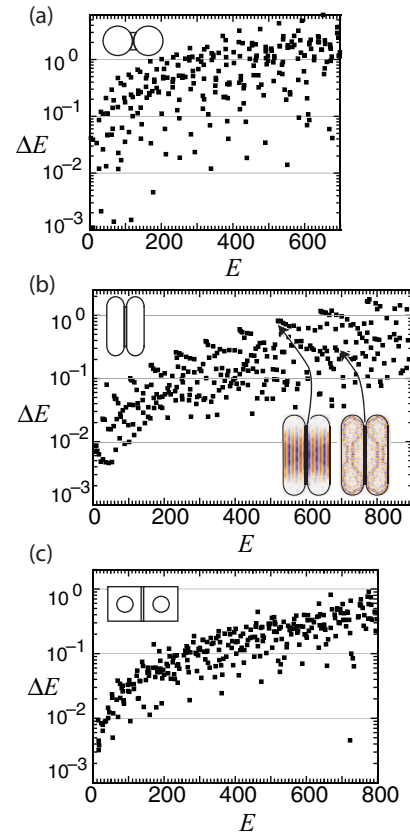


FIG. 3. (Color online) Tunneling rates for various two-dimensional wells. Tunneling rates for (a) circular, (b) stadium, and (c) Sinai-shaped systems. Insets show the double-well and barrier configuration (not to scale) and some typical eigenstates. Other chaotic well shapes (butterfly and various concave-sided wells) also show the same regularization of tunneling rates. Roughly speaking, as the systems become more chaotic, the tunneling rate variation falls drastically.

chaotic case: Each  $\Delta E$  calculated from (1) involves an average over the rectangular well  $\Delta E$  values of  $\Delta_m$  using the randomly fluctuating weights  $w_m$ . Thus we expect that fluctuations of the chaotic  $\Delta E$  values will be reduced by this averaging by a factor of the order of  $1/\sqrt{m_*} \sim 1/\sqrt{kL}$  as compared to the case of the rectangle. Therefore, we can think of the reduced fluctuations in the chaotic case as due to self-averaging over angle done by each *individual* chaotic eigenmode, and this contrasts with the rectangle case, where each mode corresponds to a single incidence angle, i.e.,  $\Delta E = \Delta_m$ .

We now test our model (1) for its prediction of fluctuation properties of the splittings. To do this, we consider the quantity  $\delta E = \Delta E - \langle \Delta E \rangle$  where  $\langle \dots \rangle$  denotes the sliding average, and we form  $\delta E$  for each energy of a data point in Fig. 1(b). Next, we compute  $\sigma_{\Delta E}^2 = \langle (\delta E)^2 \rangle$  using the same sliding window procedure as for  $\langle \Delta E \rangle$ . The resulting values of  $\sigma_{\Delta E}$  are shown as the black curve in Fig. 2(c). Next we generate  $10^4$  pseudodata realizations, and from each such set we determine  $\sigma_{\Delta E}$ . Averaging over these  $10^4$  realizations, we obtain the red curve in Fig. 2(c). In addition, we obtain the standard deviation of our set of  $10^4$  pseudodata realizations from the red curve, which we have plotted as error bars on the red curve. We see that the black and red curves are consistent to within the error

bars, as would be expected if Eq. (1) is a valid statistical model for the splitting fluctuations. For comparison, we also plot in Fig. 2(c) the result for  $\sigma_{\Delta E}$  obtained using the rectangle data of Fig. 1(a) (blue curve).

Our considerations here can also be applied to other situations. For example, we expect that similar fluctuation behavior will result when a *single* well is coupled through a tunneling barrier to an unbounded region. In this case, the lifetime of states within the well (inverse of the imaginary part of the energy level) should display the same type of chaos regularization of fluctuations seen in Fig. 1(c).

With the general view of the random-plane-wave tunneling theory in place, we now understand results for other systems which range from integrable to strongly chaotic. In Fig. 3(a), results for circular wells show a similar range of strongly fluctuating tunneling as in the rectangular well case. Here the angular momentum is conserved, and this leads to similar behavior as in the rectangle.

In Fig. 3(b)—stadium-shaped wells—we begin to see changes in the variations of tunneling rates. Notably absent in the higher energy states ( $>150$ ) are the smallest rates common in Fig. 1(a) and Fig. 3(a). This is because of the absence of states with maximal  $p_y$  momentum which results from the curved ends of the stadia destabilizing that family of orbits. Some remnants of the lines of higher tunneling rates for the rectangular wells are still evident. The latter can be traced to the family of neutrally stable periodic orbits of maximal  $p_x$  magnitude. One of the insets shows an example of a wave function of that kind called a scarred state [8].

The Sinai well shown in Fig. 3(c) shows more contraction of the energy variation beyond that of the stadium case. The high lines of tunneling rates are absent and the overall maximum variability is now down to about an order of magnitude. In the Sinai billiard there are still a considerable number of neutrally stable periodic orbits.

We note that we have concentrated on symmetric well structures since the energy splittings come about purely from tunneling, and in that way we do not have a more complicated situation of asymmetric wells where it is hard to gauge the origin of the splitting. However, we expect that in open, asymmetric systems the lifetimes of the states (essentially the resonances remaining from the closed system) will follow the same distribution as for the symmetric closed shapes. Some

preliminary calculations using our random-plane-wave theory for escape from an open system through a barrier for an integrable and nonintegrable shape show that the lifetimes of the states (essentially the resonances remaining from the closed system) follow the same distribution as for the symmetric closed shapes.

Our results suggest that tunneling currents may appear noisier in quantum devices with regular shapes where even a narrow energy window encompasses vastly different tunneling rates than in chaotic wells. Furthermore, it may be possible to engineer well shapes that assure certain tunneling rates in some windows of the energy spectrum. One could now change tunneling rates by changing the device shape, rather than by barrier height adjustment. This could be useful in devices which operate just below or in the semiclassical limit, since certain 2D quantum dot and graphene systems already operate in this regime. For example, single electron devices and solid state lasers whose operation relies on tunneling could be designed with shapes that enhance or suppress their operation, perhaps in real time if the shapes are defined electrostatically. However, we note that in open systems the situation is more nuanced. The size, orientation, and placement of channels interact with the structure of the closed system's eigenstates to affect conductances [9]. These lead to enhancements and suppression of conductances via resonances (e.g., resonance trapping) which, along with our work here, suggests their roles in regular vs chaotic cavities deserve more study.

Our results also open up several theoretical questions. Do all integrable systems have tunneling rate fluctuations which increase with energy? Our numerical results show this is true for rectangular, circular, and elliptic shapes, but we know of no theoretical proofs of this behavior. Do completely chaotic systems have tunneling rate fluctuations which eventually decrease with energy? Our random-plane-wave theory strongly suggests this, but again, we know of no proof.

In summary, we have presented strong evidence that tunneling rates for classically chaotic quantum states are semiclassically regularized to have relatively small local fluctuations with energy. This contrasts with integrable systems which suffer from very large fluctuations in tunneling rates.

This work was partly supported by ONR Grant No. N00014-07-1-0734

- 
- [1] F. Haake, *Quantum Signatures of Chaos* (Springer-Verlag, Berlin, 2001).
- [2] M. W. Beims, V. Kondratovich, and J. B. Delos, *Phys. Rev. Lett.* **81**, 4537 (1998); S. C. Creagh and N. D. Whelan, *ibid.* **82**, 5237 (1999); *Ann. Phys.* **272**, 196 (1999); J. D. Hanson, E. Ott, and T. M. Antonsen, *Phys. Rev. A* **29**, 819 (1984); M. J. Davis and E. J. Heller, *J. Chem. Phys.* **75**, 246 (1984); M. Sheinman, S. Fishman, I. Guarneri, and L. Rebuzzini, *Phys. Rev. A* **73**, 052110 (2006); S. Tomsovic (World Scientific, Singapore, 1998); S. Tomsovic and D. Ullmo, *Phys. Rev. E* **50**, 145 (1994); M. Wilkinson and J. H. Hannay, *Physica D* **27**, 201 (1987); W. K. Hensinger *et al.*, *Nature* **412** (6842), 52 (2001); D. A. Steck, W. H. Oskay, and M. G. Raizen, *Science* **293** (5528), 274 (2001).
- [3] S. Löck, A. Bäcker, R. Ketzmerick, and P. Schlagheck, *Phys. Rev. Lett.* **104**, 114101 (2010).
- [4] M. V. Berry, *J. Phys. A* **10**, 2083 (1977).
- [5] B. Batistic and M. Robnik, *J. Phys. A* **43**, 215101 (2010); F. Leyvraz and D. Ullmo, *ibid.* **29**, 2529 (1996); G. Vidmar *et al.*, *ibid.* **40**, 13883 (2007).
- [6] E. Ott, *Chaos in Dynamical Systems* (Cambridge University Press, Cambridge, United Kingdom, 1995).
- [7] M.-J. Lee, E. Ott, T. M. Antonsen, L. Pecora, D.-H. Wu, and H. Lee (unpublished).
- [8] E. J. Heller, *Phys. Rev. Lett.* **53**, 1515 (1984).
- [9] R. G. Nazmitdinov, K. N. Pichugin, I. Rotter, and P. Šeba, *Phys. Rev. B* **66**, 085322 (2002); R. G. Nazmitdinov, H.-S. Sim, H. Schomerus, and I. Rotter, *ibid.* **66**, 241302 (2002).